JOURNAL OF MATERIALS SCIENCE 21 (1986) 947–952

Changes in the kinetics of the vaterite–calcite transformation with temperature and sample crystallinity

C. BARRIGA, J. MORALES, J. L. TIRADO
Departamento de Química Inorgánica, Facultad de Ciencias, Universidad de Córdoba, Córdoba 14005, Spain

The effect of temperature and crystallinity on the kinetics of the vaterite–calcite thermal transformation has been examined by analysis of isothermal data evaluated by X-ray diffraction techniques and differential scanning calorimetry. These results were compared with dynamic differential scanning calorimetry results and complemented by X-ray line profile analysis and scanning electron microscopy studies. In the 445 to 485°C temperature range, the kinetic data can be fitted reasonably well to a phase-boundary equation. At higher temperatures (510 to 530°C) by using differential scanning calorimetry techniques, an Avrami equation describes more accurately the conversion curves and a decrease in activation energy is observed. This change in the formal mechanism is supoported by the external morphology of the particles, revealed by scanning electron microscopy. Prior mechanical treatment of vaterite causes an increase in activation energy, due to the recrystallization process that accompanies the reaction.

1. Introduction

The technological applications of calcium carbonate are diverse and require the preparation of materials with different physical and chemical properties. The formation and interconversion of the different $CaCO_3$ phases have been extensively investigated for the characterization of the mechanism involved in the transformations and the properties of the reaction products. On the other hand, the influence of prior mechanical treatment by grinding procedures in the reactivity of solids deserves great interest as it may induce significant alterations in the surface and bulk properties of solids and in the mechanism of the transformation.

The kinetics of the vaterite–calcite phase transition promoted by thermal treatment have been examined by several authors. Rao [1] proposed a contracting sphere mechanism for the complete course of the reaction and computed a value of activation energy of 397 kJ mol^{-1} by the analysis of isothermal data while a value of 502 kJ mol^{-1} was obtained by the application of the method of Borchardt and Daniels [2] to differential thermal analysis (DTA) traces. Additionally, Rao [1] suggested that a break up of the particles during the transformation was responsible of a change in slope of the plots of the $\frac{2}{3}$ power law. However, the data to support this assumption were not reported.

In a more recent paper, Davies *et al.* [3] studied the kinetics of this transformation from the analysis of an endothermal effect in the DTA curve. As this reaction is clearly exothermic, little attention should be paid to their results.

The differences found in the kinetic results obtained from under isothermal and dynamic conditions can be explained in terms of the difficulty in obtaining unambiguously evaluable kinetic results from DTA experiments [4] and/or a change in the mechanism with temperature.

In the last few years, it has been pointed out [5–7] that differential scanning calorimetry (DSC) is a useful tool for the determination of kinetic parameters, specially for reactions in which no weight loss is detected. In most cases, a single-temperature programmed DSC experiment has been used to study the kinetics of the reaction, but little attention has been paid to the comparison of the non-isothermal results with those computed from isothermal conditions, which can be performed by DSC.

In the present paper, the kinetics of the vaterite–calcite phase transition have been examined by using X-ray analysis for the estimation of the relative amount of phases converted and by the application of DSC techniques under isothermal and non-isothermal conditions. A comparative study of these methods has been developed to assess their validity and usefulness and the time–temperature dependence of the reaction has been investigated.

Another goal of this paper is to examine the influence of preliminary mechanical treatment on the kinetics of the phase transition. In this way, the effect of grinding on the thermal behaviour of vaterite has been recently reported [8] and the crystallinity of the samples was found to originate significant changes in the DSC traces.

2. Experimental techniques

Synthetic vaterite was prepared by the method described by Rao [1]. A portion of this sample was

0022–2461/86 $03.00 + .12

ground for 7 h in a Fritsch ME 030177 planetary mill equipped with a 80 ml cylindric agate mortar and three balls 10 mm diameter of the same material. The charge of vaterite was 10 g.

Isothermal runs were carried out in a furnace provided with a chromel/alumel thermocouple and temperature control. The degree of conversion at fixed time intervals was evaluated by quantitative analysis of powder X-ray diffraction patterns by the method proposed by Rao [1] and the autoflushing model proposed by Chung [9]. According to Chung for any binary system an autoflushing phenomenon emerges and each component flushes out the mass absorption coefficient of the other of the intensity-concentration equation.

Differential scanning calorimetry was used to obtain isothermal runs at higher temperatures and dynamic traces of the exothermal effect of the phase transition. The measurements were carried out in a Mettler TA 3000 system under static air atmosphere and sample weights of ~25 mg. The traces were digitalized by a Calcomp 2000 apparatus and converted into degree of conversion by numerical integration.

The X-ray diffraction patterns were obtained with a Philips PW 1130 diffractometer provided with Co$K\alpha$ radiation and an iron filter. Line profiles were recorded at 0.125° 2θ min^{-1}. The evaluation of crystallite size and microstrains was performed by the variance method [10], performing the corrections pointed out by Langford [11].

The electron micrographs were obtained with a Philips SEM 501 B. Samples were placed in nickel holders and covered with electrodeposited gold for their examination.

3. Results and discussion

The temperature interval used for the study in isothermal conditions by the application of X-ray quantitative analysis was 445 to 485° C. Fig. 1 shows a plot of these data obtained by the autoflushing method. For comparison, the data evaluated at 485° C by the method of Rao [1] are also included. Although both methods yield similar results, some divergences are observed at high values of degree of conversion, α,

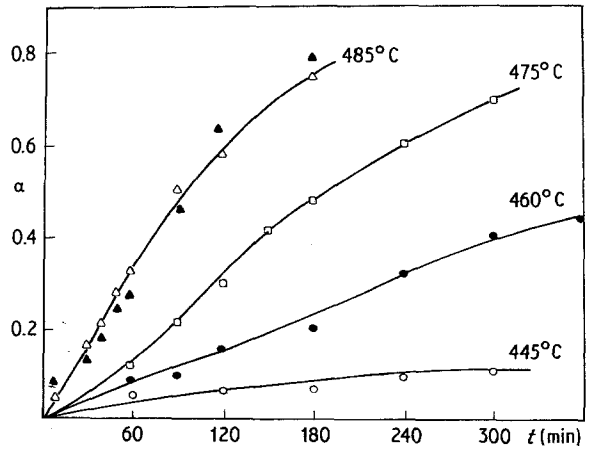

Figure 1 Degree of conversion against time plots, evaluated by X-ray diffraction quantitative analysis. (△) Autoflushing and (▲) Rao [1], at 485° C, (□) 475° C, (●) 460° C, (○) 445° C.

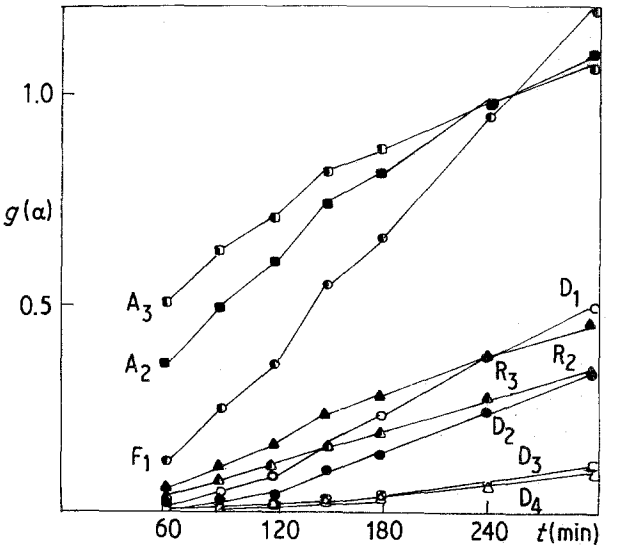

Figure 2 $g(\alpha)$ against time plots for the kinetic data at 485° C.

probably due to the overlapping of the 1 1 2 and 0 0 6 reflections of calcite, which are not considered in the autoflushing process. The α-time curves have an initial induction period which is either very small or virtually absent.

These data were analysed by obtaining the plots of $g(\alpha)$ against t (Fig. 2), according to the kinetic expression in Table I. From these plots, the rate constants and regression coefficients r, were obtained by fitting these data to a straight line, according to the expression:

$$g(\alpha) = kt \qquad (1)$$

where k is the rate constant of the reaction. The r values were compared by the statistical t test of significance [12] from which some of the kinetic laws could be discarded (mainly A_2 and A_3) at a 99.99% confidence level. However, a single mechanism could not be chosen. In this way, Brown and Galway [13] have questioned the value of regression coefficients to discriminate the true law.

The rate constants were used to obtain the Arrhenius plots for each mechanism (Fig. 3) and the values of activation energy shown in Table II. It should be noted that the activation energies are dependent on the kinetic expression used in the analysis with values ranging from 255 to 577 kJ mol^{-1} and the corresponding regression coefficients allowed no further discrimination of kinetic laws.

From the above results, it can be derived that the

TABLE I List of algebraic functions $g(\alpha)$ used in the kinetic analysis

Symbol	Model	$g(\alpha)$
F_1	First-order	$-\ln(1-\alpha)$
A_2	Nucleation (Avrami)	$[-\ln(1-\alpha)]^{1/2}$
A_3	Nucleation (Erofeev)	$[-\ln(1-\alpha)]^{1/3}$
R_2	Contracting area	$1-(1-\alpha)^{1/2}$
R_3	Contracting sphere	$1-(1-\alpha)^{1/3}$
D_1	One-dimensional diffusion	α^2
D_2	Two-dimensional diffusion	$(1-\alpha)\ln(1-\alpha)+\alpha$
D_3	Three-dimensional diffusion	$[1-(1-\alpha)^{1/3}]^2$
D_4	Ginstling–Brounshtein	$(1-2\alpha/3)-(1-\alpha)^{2/3}$

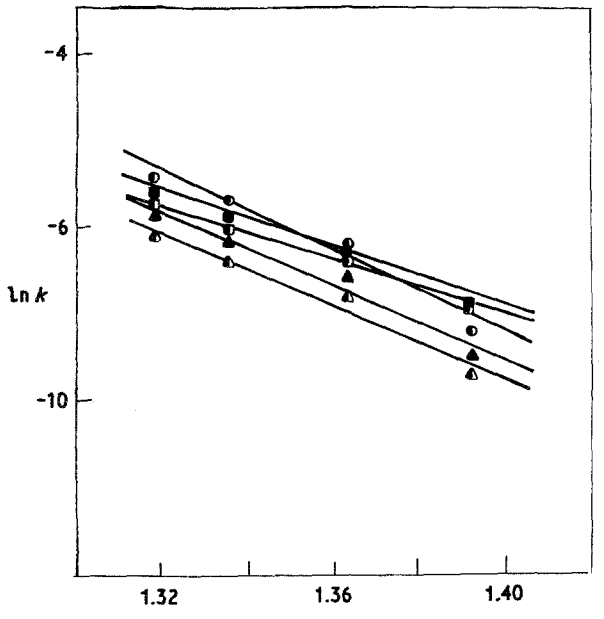

Figure 3 Arrhenius plots of low temperature kinetic data for several selected expressions. (◐) F_1, (■) A_2, (◘) A_3, (▲) R_2, (▲) R_3.

formal analysis of kinetic data cannot be used to discern the true mechanism governing the transformation at these temperatures. The application of parallel techniques may give new light. In this way, the electron micrographs of the original vaterite sample and the transformation product are shown in Fig. 4. It can be observed that particle shape is not altered in the process of conversion in contrast with the results of Rao [1]. This fact may indicate that the change observed in the slope of the plot of the contracting sphere equation (R_3) should not be considered adequate. Indeed, our results do not support the behaviour found by Rao as indicated in Fig. 2, in which no change in slope is observed in the $g(\alpha)$ against t plots for an R_3 mechanism or any other. Moreover, the absence of cracks or fractures in the particles (Fig. 4b) suggest that the strains induced by the misfit of the structures of calcite and vaterite are unimportant, as discussed below.

These observations are complemented by the results of the line profile analysis shown in Table III. The values of crystallite size and microstrains computed by the variance method from the 1 0 4 reflection of calcite show that the coherently diffracting domains increase their size immediately after the occurrence of this phase while microstrains decrease simultaneously.

TABLE II Results of the kinetic analysis of isothermal data

Kinetic law	Low-temperature X-ray data, E (kJ mol^{-1})	High-temperature DSC data, E (kJ mol^{-1})	
		Unground	Ground for 7 h
F_1	387	449	329
A_2	279	324	333
A_3	254	283	312
R_2	349	329	345
R_3	358	366	349
D_1	495	354	358
D_2	532	437	387
D_3	574	570	437
D_4	545	487	404

The growth of calcite domains and the progressive accommodation of the structures of calcite and vaterite may cause this behaviour.

On the other hand, the analysis of the 1 1 0 and 1 1 1 lines of vaterite, also shown in Table III, show a similar evolution at low heating periods. For this phase, the increase in crystallite size should be explained in terms of an intragranular sintering process throughout the transformation, which is limited by the growth of calcite domains, as indicated by the less pronounced increase after 2 h and the diminution from 4 to 6 h.

The formal kinetic analysis was also carried out in isothermal DSC traces obtained in the temperature interval 510 to 530° C. This narrow interval was imposed by the equipment sensitivity and the high rates of decomposition above 530° C. Similar limitations can be found in other studies [5]. The DSC traces collected in Fig. 5 were used to obtain the α values by numerical integration, rate constants and the values of activation energy. The latter are also included in Table II. The variability of these results with the formal kinetic law is also significant.

Additionally, the $\ln [-\ln(1 - \alpha)]$ against $\ln t$ plots were applied to both types of isothermal data (Fig. 6). This method implies the least-squares fitting of the data to the expression:

$$\ln [-\ln (1 - \alpha)] = n \ln k + n \ln t \qquad (2)$$

where n is the exponent in the Avrami law. Some interesting aspects are revealed by these plots. First, a marked increase in slope is observed as the temperature of the isothermal experiment is higher. For the DSC isotherms, the value of n computed from the slope was 2.6 ± 0.3 while an average value of 1.3 ± 0.1 was calculated from the isothermal data recorded at the interval 445 to 485° C. These results suggest a change in the mechanism of the phase transition with temperature.

According to Hancock and Sharp [14], values of n of 2 and 3 correspond to the Avrami equations A_2 and A_3, respectively, while values closer to unity can be interpreted by a phase-boundary controlled reaction (R_2 or R_3).

TABLE III Crystallite size (ε_k) and microstrains ($\langle e^2 \rangle^{1/2}$) computed by the variance method for 1 1 0 and 1 1 1 lines of vaterite and the 1 0 4 line of calcite

Heating time (h)	hkl	ε_k (nm)	$10^3 \langle e^2 \rangle^{1/2}$
0	1 1 0	14.9	2.1
	1 1 1	20.6	2.2
2	1 0 4	87.9	1.0
	1 1 0	30.7	1.6
	1 1 1	32.1	1.9
4	1 0 4	117	0.5
	1 1 0	37.1	1.1
	1 1 1	36	1.8
6	1 0 4	560	–
	1 1 0	36	1.2
	1 1 1	33.5	1.6
Sample ground for 7 hours	1 1 0	14.7	2.0
	1 1 1	18.1	3.0

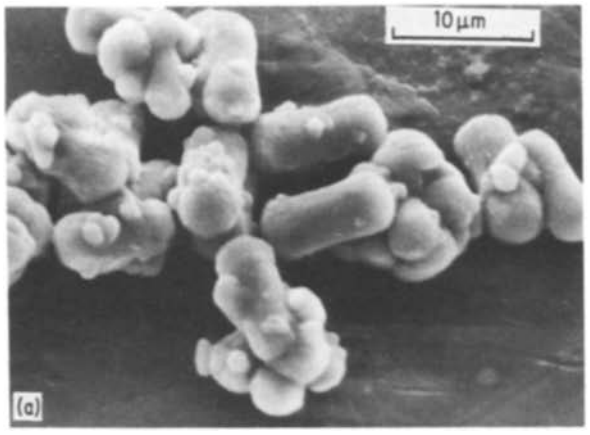

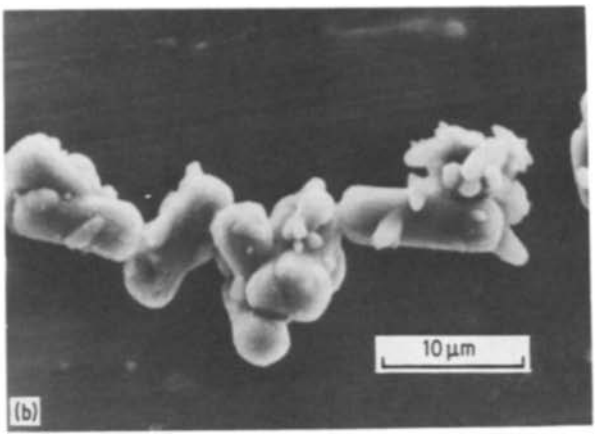

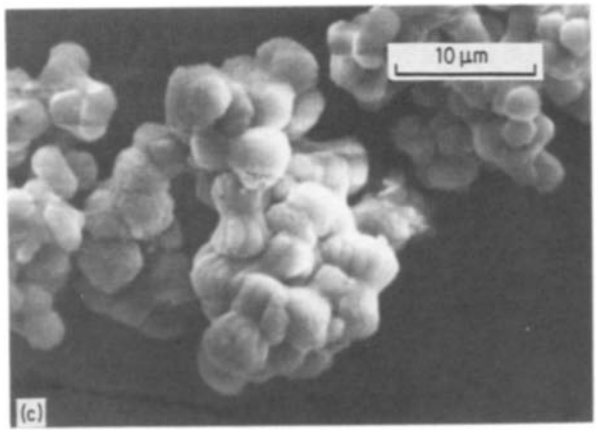

Figure 4 Scanning electron micrographs of (a) original vaterite, (b) product of the low-temperature isotherms, and (c) product of a high-temperature DSC isotherm.

In addition to the ln–ln plots, the values of activation energy support this interpretation. In the low temperature region, the reaction progresses slowly and this fact is reflected in the value of the activation energy (349 to 358 kJ mol^{-1}) for the nucleation and advance of the interface inwards towards the particle. When the temperature increases, the activation energy found with a mechanism described empirically by the Avrami law with exponent of 2.5 is 270 kJ mol^{-1}. These data may be interpreted by considering that under these conditions, the observed activation energy represents the activation energy required for the rate of propagation, since the induction period is negligible.

A final proof of these changes can be obtained by comparing the size and shape of the particles of the product obtained in both temperature intervals. In this way, Fig. 4c includes an electron micrograph of the sample derived from a DSC trace recorded at 520°C. The most relevant difference with respect to Fig. 4b is a change in the external shape of the particles and a decrease in their size. The peanut-like shape has been distorted by a shrinkage in a plane which is at the centre of the particle, perpendicular to the longer axis. The alteration yields spherulitic shapes

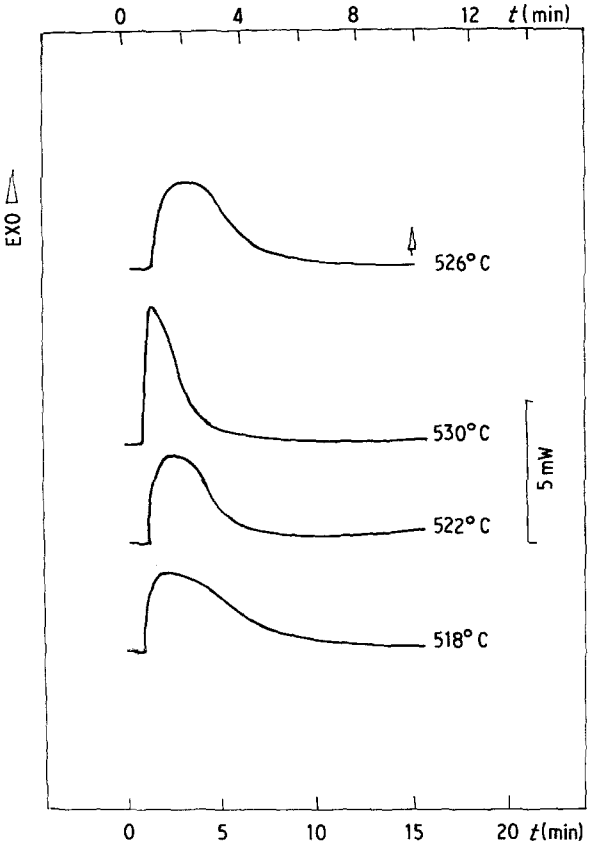

Figure 5 Isothermal DSC curves in the temperature interval 518 to 530° C.

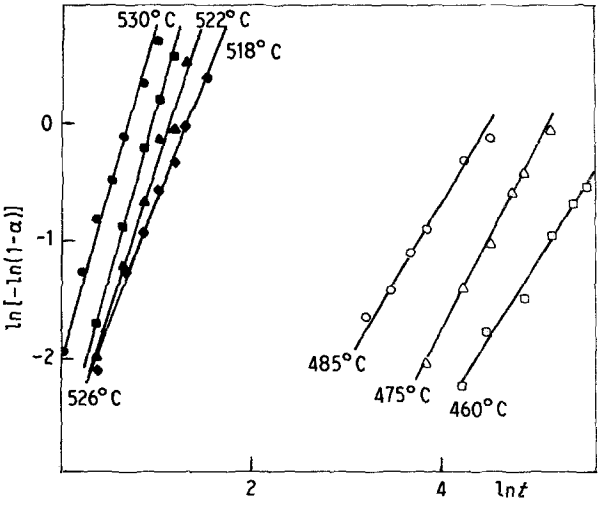

Figure 6 ln [− ln (1 − α)] against ln t plots for the isothermal runs.

TABLE IV Values of activation energy (kJ mol^{-1}) computed from the analysis of dynamic DSC traces

Kinetic law	Coats and Redfern [16]			Achar *et al.* [17]
	3° min^{-1}	8° min^{-1}	13° min^{-1}	3° min^{-1}
F_1	905	587	570	1040
A_2	445	287	279	582
A_3	291	188	180	429
R_2	778	508	487	770
R_3	816	533	512	857
D_1	1356	894	853	1190
D_2	1490	978	936	1420
D_3	1647	1082	1040	1689
D_4	1539	1015	969	1510

similar to those found by Sohnel and Mullin [15], and the surface seems to be formed by smaller particles clustered together. This picture agrees fairly well with the differences found in the formal kinetic analysis.

When the reaction develops slowly, the formation of an interface and its advance from the surface towards the centre prevents the break-up of the particles. In contrast, when the reaction is followed by DSC, a bulk nucleation process takes place and the subsequent fast growth of these nuclei may cause the internal rupture of the particle, which is indicated in their external texture.

Finally, non-isothermal methods of kinetic analysis were applied to dynamic DSC traces. Three runs were performed at 3, 8 and 13° min^{-1}, converted into α-T plots and analysed by means of the Coats and Redfern [16] and Achar *et al.* [17] methods.

The results obtained by both methods are summarized in Table IV. The dependence of the kinetic parameters on heating rate is indicated by the higher values of activation energy at lower heating rates. This behaviour has been also found in other studies [12] and a complete agreement with conclusions based upon isothermal results can be achieved by reducing the heating rate of the dynamic experiment.

If the results of Table IV at 3° min^{-1} are compared with those in Table II, the best agreement is obtained for an A_3 mechanism in the DSC isotherms, while the remaining kinetic expressions show important divergences. This is in agreement with a random nucleation process followed by a three-dimensional growth of nuclei mechanism. On the other hand, the comparison of low temperature isothermal results (Table II) with the results in Table IV does not allow the selection of a single mechanism. This fact can be explained on the basis of the change in mechanism discussed above, by considering that the dynamic runs cause the transformation to proceed according to the same kinetic law as in high-temperature isothermal runs.

The method of Achar *et al.* was applied to the 3° min^{-1} run. The kinetic parameters evaluated by this procedure (see Table IV) show important deviations from the method of Coats and Redfern. Moreover, they show divergences for the parameters evaluated by the isothermal procedures. Although the regression coefficients of an A_3 mechanism are high, the values of activation energy are always much higher. Probably, these divergences are due to the evaluation of the height of the peaks which is highly dependent on the choice of baseline.

The effect of vaterite crystallinity on the kinetics of its transformation to calcite was studied by the analysis of several isothermic DSC curves of a vaterite sample ground for 7 h. A small amount of calcite ($\sim 10\%$) was present in this sample originated by the mechanical treatment [8]. The values of crystallite size and microstrains for this sample are included in Table III and show a lower crystallite size as compared with the original vaterite (0 h thermal treatment).

The values of activation energy obtained from the Arrhenius plots with the rate constants calculated from the analysis of isothermal DSC traces in the temperature range 518 to 530°C are shown in Table II. The slope of the ln–ln plots was 2.4 ± 0.3 which suggests that an Avrami mechanism is also valid for this sample. However, the corresponding activation energy (see Table II) is approximately 30 kJ mol^{-1} higher as compared with the unground sample. This change can be considered significant as the standard deviation in the repeatability of the determination of this parameter was estimated to be 3%. Similar deviations have been recently found in other studies [7]. This change may be interpreted in the light of the recovery of crystallinity that accompanies the phase transition [8]. In this way, the activation energy of the ground sample can be considered to be sum of the activation energies corresponding to both processes. It should be emphasized that the impossibility of separating these processes implies that the kinetic parameters computed in the analysis and discussed above unavoidably involve both phenomena. A similar conjunction has been found in ground litharge in respect to its transformation to massicot [18].

4. Conclusions

From the above discussion, it can be concluded that the results of the formal kinetic analysis of the thermal transformation vaterite–calcite are markedly influenced by the temperature interval used in the analysis. While a phase-boundary equation describes the low-temperature isothermal runs, dynamic and high temperature isothermal runs are better described by an Avrami equation. The electron microscopy observations reveal a change in the particle morphology as the temperature of the phase transformation increases. Finally, the preliminary mechanical treatment causes a slight increase in activation energy but no alteration in the mechanism can be deduced.

Acknowledgement

This work was carried out with the financial support of CAICYT (contract 0608/81).

References

1. M. S. RAO, *Bull. Chem. Soc. Jpn.* **46** (1973) 1414.
2. H. BORCHARDT and F. DANIELS, *J. Amer. Chem. Soc.* **79** (1957) 41.
3. P. DAVIES, D. DOLLIMORE and G. R. HEAL, *J. Thermal Anal.* **13** (1978) 473.
4. J. MORALES, L. HERNAN, M. MACIAS and A. ORTEGA, *J. Mater. Sci.* **18** (1983) 2117.
5. N. P. BANSAL, R. H. DOREMUS, A. J. BRUCE and

C. T. MOYNIHAN, *J. Amer. Ceram. Soc.* **66** (1983) 223.
6. M. T. CLAVAGUERA-MORA, S. SURIÑACH, M. BARO and C. CLAVAGUERA, *J. Mater. Sci.* **18** (1983) 1381.
7. J. C. M. TORFS, L. DEIJ, A. J. DORREPAAL and J. C. HEIJENS, *Anal. Chem.* **56** (1984) 2863.
8. C. BARRIGA, J. MORALES and J. L. TIRADO, *J. Mater. Sci.* **20** (1985) 941.
9. F. H. CHUNG, *J. Appl. Cryst.* **7** (1974) 519.
10. J. I. LANGFORD and A. J. C. WILSON, in "Crystallography and Crystal Perfection", edited by G. N. Ramachandran (Academic Press, London, 1963) p. 207.
11. J. I. LANGFORD, *J. Appl. Cryst.* **15** (1982) 315.
12. L. HERNAN, J. MORALES, A. ORTEGA and J. L. TIRADO, *J. Thermal Anal.* **29** (1984) 479.
13. M. E. BROWN and A. K. GALWAY, *Thermochim. Acta* **29** (1979) 129.
14. J. D. HANCOCK and J. H. SHARP, *J. Amer. Ceram. Soc.* **55** (1972) 74.
15. O. SOHNEL and J. W. MULLIN, *J. Cryst. Growth* **60** (1982) 239.
16. A. W. COATS and J. P. REDFERN, *Nature* **201** (1964) 68.
17. B. N. N. ACHAR, G. W. BRINDLEY and J. H. SHARP, in Procedings of the International Clay Conference, Jerusalem, 1966, edited by L. Heller and D. Weiss (Israel Program for Scientific Translations, Jerusalem, 1966) p. 67.
18. J. MORALES, J. L. TIRADO, M. MACIAS and A. ORTEGA, *React. Solids* **1** (1985) 43.

Received 18 March
and accepted 30 May 1985